persists in the dorsal regions of the embryo from the neural plate caudally to the regressing blastopore. Staining extends around the blastopore but expression appears to subside on the ventral surface (Figure 16I-Q). Inspection of whole mount specimens revealed definitive staining in the surface ectoderm, neural tube and somites. As the embryo develops, the posterior, ventral regions lose *Xbves* expression and message levels become progressively restricted to the heart, somites, cement gland, and eyes by stage 35.

A recent study reported that *Xbves/pop1a* whole mount hybridization was restricted to the heart during embryogenesis and that whole mount hybridization of early embryos was summarized as "unrevealing" (Hitz et al., 2002). Because our data greatly varied from this study, we performed whole mount analyses using three separate RNA probes from bp 70-670 (5'), 870-1210 (3') and full-length (1-1738) *Xbves*. While slight variation in intensity existed between these three groups, the same pattern of hybridization was observed over the period of development analyzed (Figure 17). It should be noted that we, like Hitz et al. (2002), observe a higher degree of hybridization in the heart at stage 35 (Figure 16Q). These data lead us to the conclusion that *Xbves* is indeed expressed in the early *X. laevis* embryo.

Immunochemical analyses were performed over the same timeframe and at later stage embryos to determine the cellular and subcellular localization of Xbves protein. The regions of positive staining corresponded to the same regions seen in whole mount hybridization (Figure 16). At these stages, most cells of the embryo are epithelial in nature and the highest levels of staining were observed at the periphery of these cells (Figure 18B,D, white arrows). Similar subcellular distribution was seen with a pan-cadherin antibody (data not shown). In the region of the blastopore at stage 11.5, both surface and involuting cells are Xbves-positive (Figure 18C, yellow arrows). At the earlier cleavage stages of embryonic development immunolocalization of

Xbves protein and other antigens was difficult using the methods we employed as well as several alternative techniques (Cordenonsi et al., 1997; Fagotto and Gumbiner, 1994; Fleming et al., 2000; Schohl and Fagotto, 2002). Positive antibody signals above background for any of the reagents we tested were not consistent or reliable in our hands at these earliest stages. During the later cleavage stages (stage 8), positive Xbves staining was observed in cells throughout the developing embryo and this reactivity is clearly above pre-immune controls (compare Figures 18A-D and 18E-F). Background nuclear staining was inconsistently observed in sectioned embryos up to stage 22 with anti-Xbves and pan-cadherin (data not shown). This nonspecific nuclear staining has been seen in published immunofluorescence studies of cleavage and gastrulation stage tissue sections (Angres et al., 1991; Heasman et al., 1994b). After this time, the nonspecific nuclear background subsided for all immunochemical reagents.

As development proceeds, surface ectoderm remains positive for Xbves as well as other ectodermal derivatives such as the eye anlage and neural tube (Figure 19A, arrowhead). Mesodermal cells, including the pseudostratified columnar epithelium of the notochord, exhibit distinct peripheral membrane staining (Figure 19B, arrow).

After stage 22, anti-Xbves staining becomes progressively restricted. The ectoderm remains positive until stage 12.5 and is greatly restricted thereafter. At these stages, an abrupt distinction between positive and negative staining can be observed at the ectodermal/endodermal junction in the mouth (Figure 20B-C). Skeletal muscle is highly positive for anti-Xbves, as are cardiac myocytes (Figure 20G-H). Later, several epithelial cell types such as the gut mucosa, epidermis, lens, cornea, retina, pronephros and velar plate express Xbves (figure 20A,D-G).

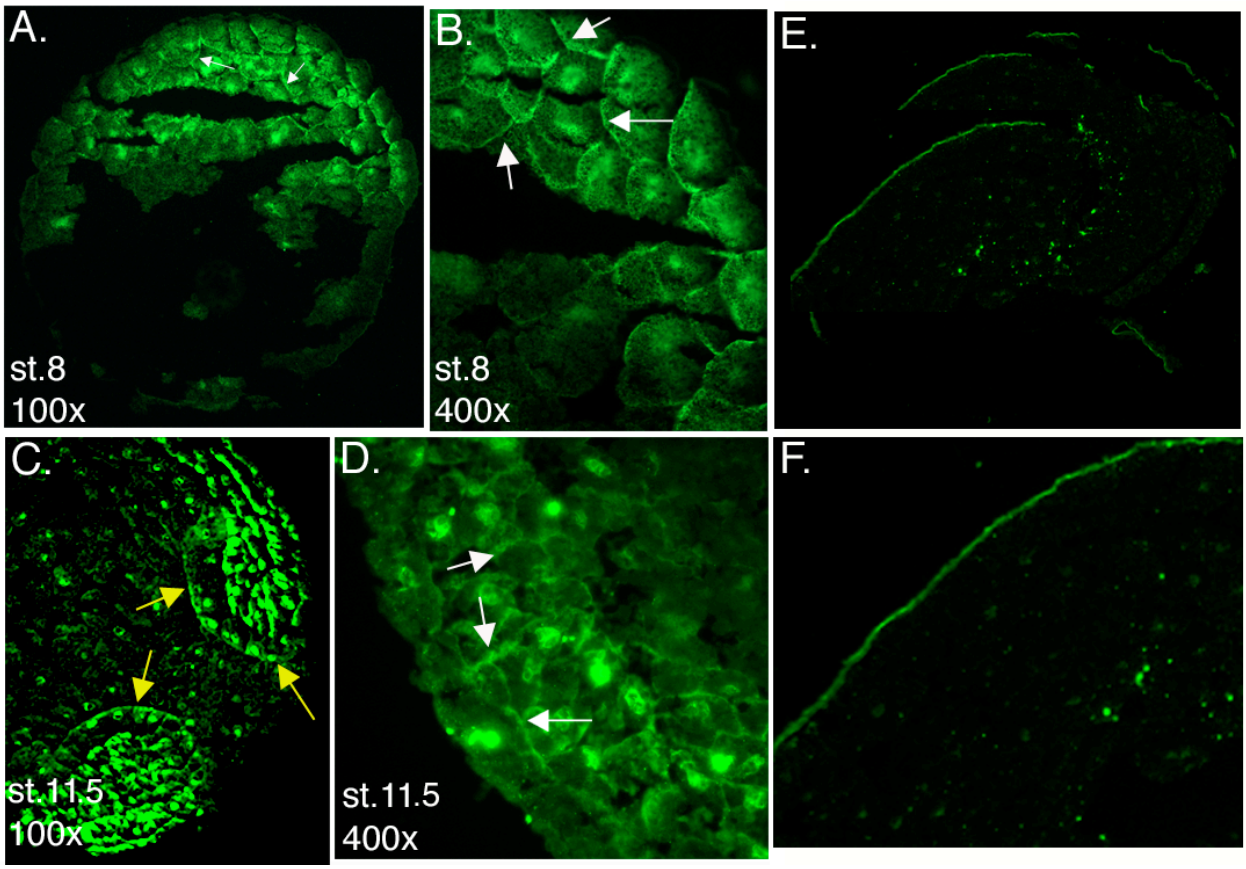

Figure 18. Immunohistochemical analysis of Xbves expression in tissue sections of *X. laevis* **embryos.** (A-B) Anti-Xbves (green) immunoreacts with protein at the cell surface (white arrows) of cleavage stage 8 embryos (A,100x; B, 400x). (C-D) Immunoreactivity of anti-Xbves in gastrulation stage 11.5 embryos is seen in the surface epithelium and involuting (yellow arrows) cells. High magnification (D) shows cell surface expression (white arrows). (E-F) Preimmune negative control of gastrulation stage embryo at 100x (E) and 400X (F).

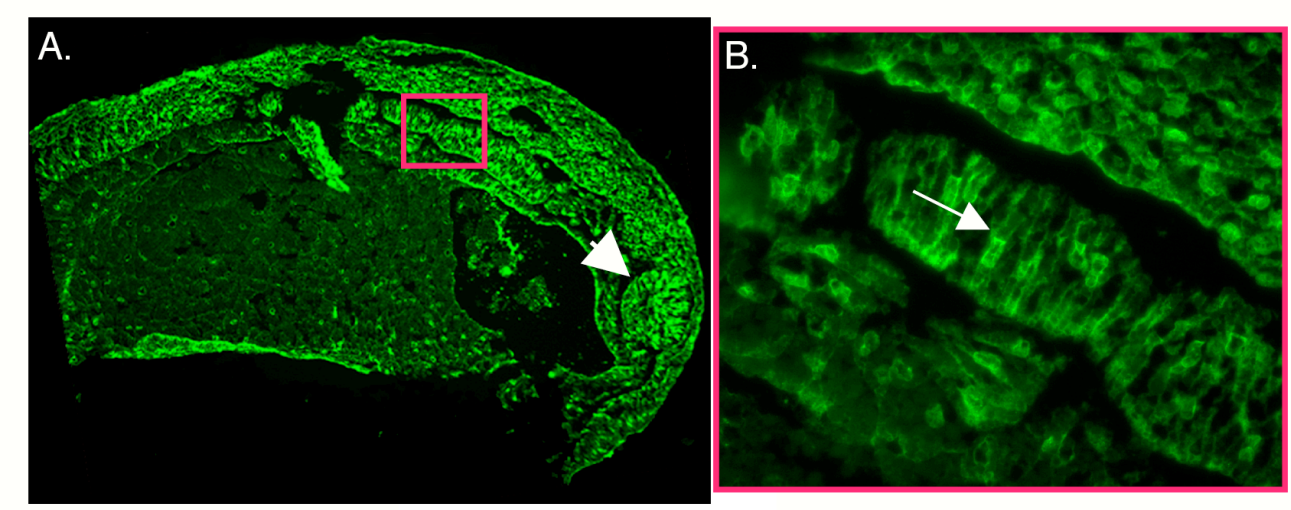

Figure 19. Immunohistochemical analysis of Xbves expression in neurulation stage embryo. (A) Anti-Xbves (green) immunoreacts with protein of a stage 19 *X. laevis* embryo in ectodermal and mesodermal tissues (40x magnification). Pink box represents image shown in (B). White arrowhead indicates Xbves expression in the eye anlage. (B) Xbves expression is detected at the cell surface (white arrow) of mesodermal derived notochord (400x magnification).

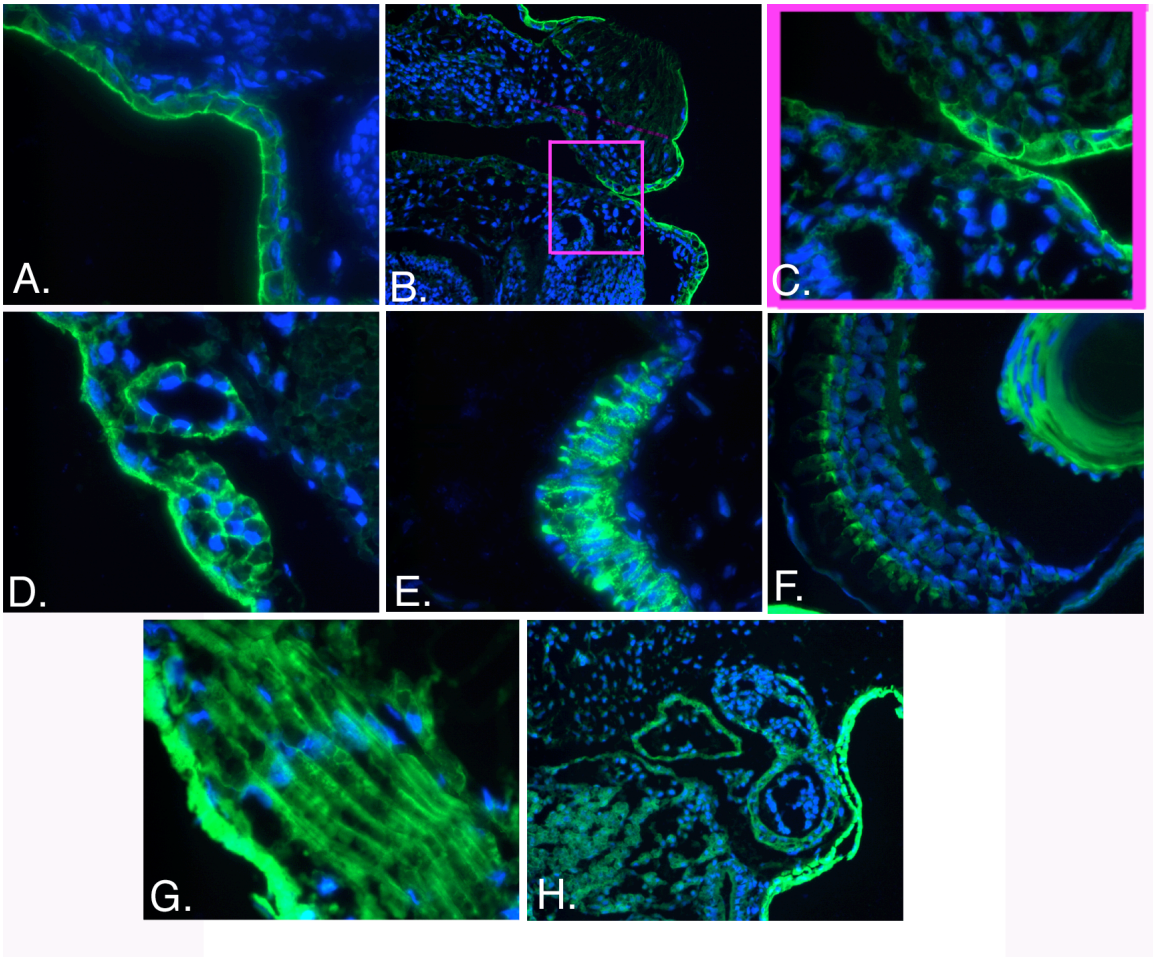

Figure 20. Immunohistochemical analysis of Xbves expression in selected *X. laevis* tadpole tissue. (A-H) Anti-Xbves (green) immunoreacts with protein in the epidermis (A), at the ectoderm-endodermal boundary of the mouth (B, 40x-C, 400x, pronephros (D), velar plate (E), lens and photoreceptors of the eye (F), skeletal muscle (G), and ventricle and atria of the heart (H). Pink box in B represents the image shown in C. DAPI nuclear stain is shown in blue.

In summary, these studies demonstrate that Xbves is expressed in most cells of the early embryo during the movement of epithelial structures. Later, Xbves staining is lost in non-epithelial cells and becomes confined to specific epithelia and striated muscle of the growing embryo.

Disruption of *Xbves* function inhibits gastrulation movements

From the preceding studies it is clear that *Xbves* is expressed during cleavage and gastrulation of the frog embryo. In an effort to determine the function of Xbves during these early phases of development, morpholino antisense oligonucleotides were designed against the *Xbves* transcript to knock down protein translation in the developing *X. laevis* embryo. The efficacy of a series of morpholinos at varying concentrations was tested by injection of three oligonucleotides against different sequences in the 5'UTR exclusively, or including the start codon and 5'coding sequence (Figure 21). Each of the three *Xbves* antisense morpholinos or a sense morpholino was injected at concentrations ranging from 10-80 ng into one or both cells of the two-cell *X. laevis* embryos. Embryos injected with doses higher than 40 ng of both the *Xbves* and the sense control morpholinos developed abnormally and thus I concluded these high concentration defects to be nonspecific. However, of the embryos injected with 30-40 ng of the *Xbves* antisense morpholinos, only the group injected with MO#1 (see Figure 21) displayed an early developmental phenotype compared to embryos injected with a sense morpholino at the same concentration or uninjected embryos. Embryos injected with comparable amounts of MO#2 and #3 developed normally; therefore, these morpholinos were considered ineffective and not furthered used. Additionally, the phenotype resulting from injection of 40ng of MO#1 can be rescued by co-injection with *Xbves* RNA lacking the morpholino target sequence denoting

specificity (discussed in greater detail below). Therefore, I have chosen to use MO#1 at a concentration of 40ng for the following experiments (A less severe phenotype is produced with lower concentrations of MO#1 and is discussed in Chapter VI).

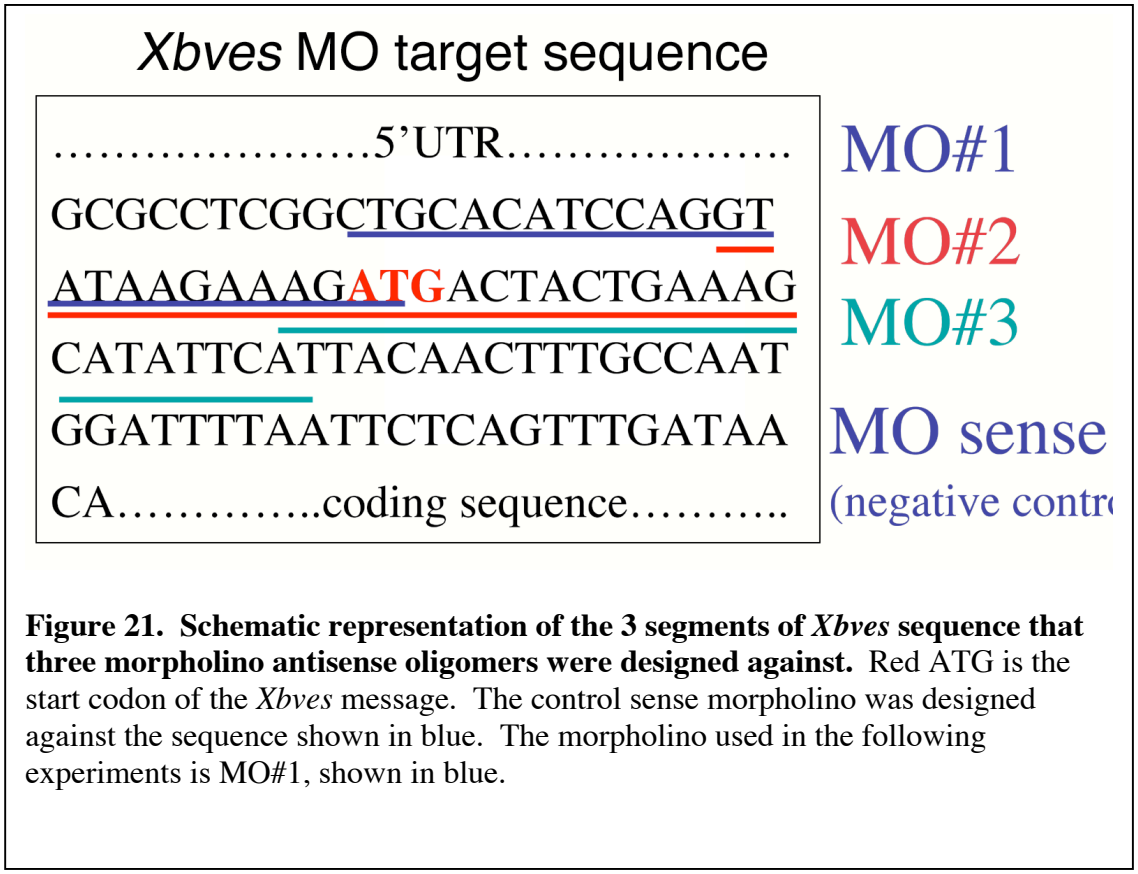

Figure 21. Schematic representation of the 3 segments of *Xbves* sequence that three morpholino antisense oligomers were designed against. Red ATG is the start codon of the *Xbves* message. The control sense morpholino was designed against the sequence shown in blue. The morpholino used in the following experiments is MO#1, shown in blue.

During cleavage stages, *Xbves* morpholino-injected embryos develop normally (Figure 22A-D), most likely because the maternally stored *Xbves* message and protein is not blocked by the morpholino oligonucleotide. Embryos develop at a similar rate and appear normal and healthy until gastrulation, when compared to sense injected or uninjected embryos. At early gastrulation, antisense morpholino-injected embryos start to form a normal dorsal blastopore lip as evident by the distinct pigment streak seen in Figure 26 (white arrow). At stage 11.5, the

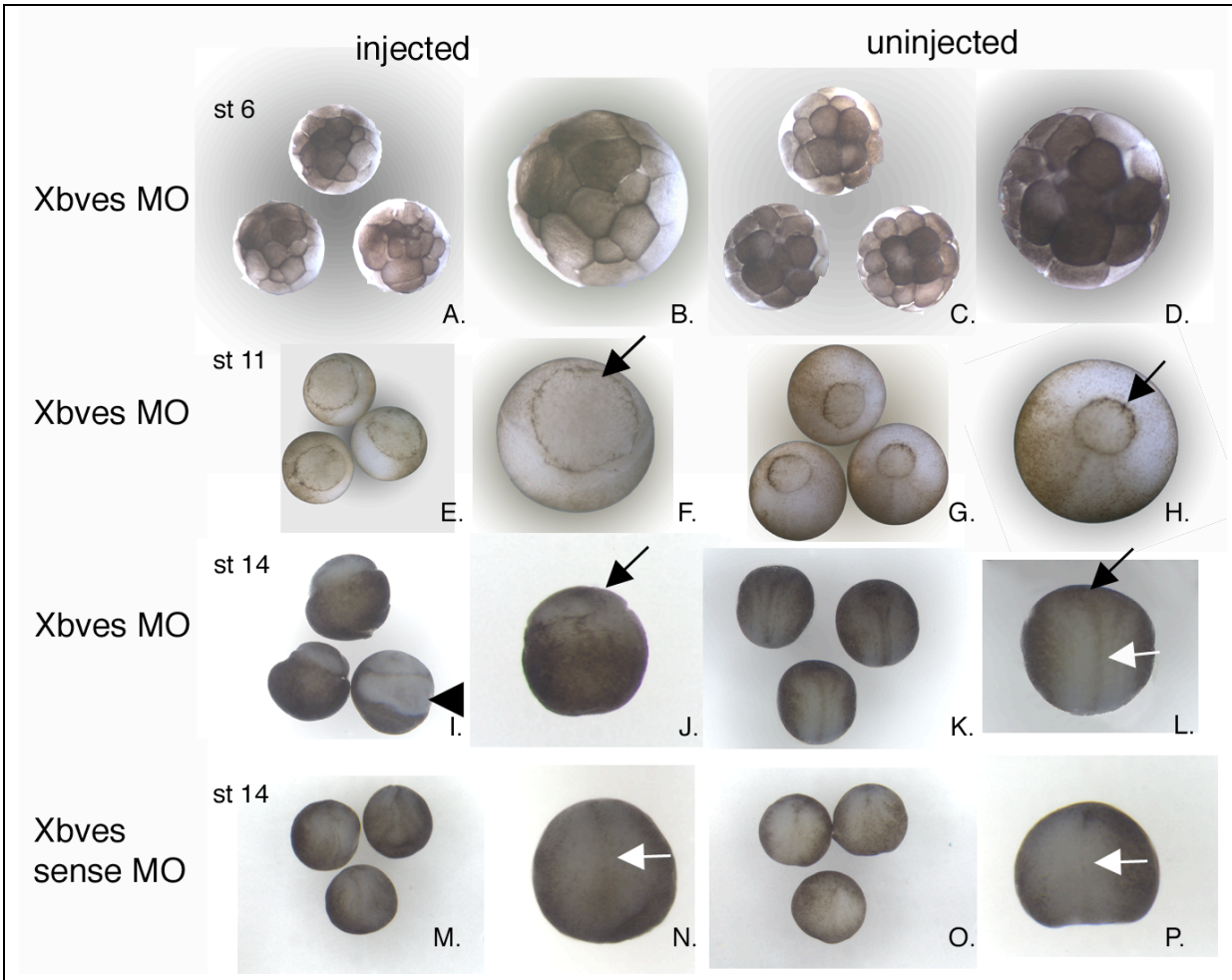

Figure 22. Injection of *Xbves* morpholino into 2-cell *X. laevis* embryos inhibits gastrulation movements. (A-D) Morpholino-injected (A-B) cleavage stage embryos develop at a similar rate compared to uninjected embryos (C-D). (E-H) Morpholino-injected embryos at stage 11 have a larger yolk plug (black arrows) than noninjected (G-H). (I-L) Stage 14 morpholino-injected embryos (I-J) have a large exposed yolk plug compared to uninjected embryos (K-L) that have a closed yolk plug (black arrows). Uninjected embryos are undergoing neurulation indicated by the neural plate (white arrow), whereas morpholino-injected embryos have no sign of neural plate formation, but rather are starting to become necrotic (black arrowhead). (M-P) Control sense morpholino-injected embryos (M-N) complete gastrulation and undergo neurulation (neural plate, white arrows), at the same rate compared with uninjected embryos (O-P).

appearance of a large yolk plug in morpholino-injected embryos indicate that the ventral blastopore lip has formed as well (Figure 22E-H). However, at this stage it is evident that the morpholino embryos have a considerably larger yolk plug signifying that the pigmented surface ectoderm has failed to cover the white vegetal cell mass when compared to the uninjected embryos. This phenotype is even more evident at post gastrulation stage 14. As seen in Figure 22I-L, uninjected embryos complete gastrulation as visualized by surface epiboly movements that cover the yolk plug and continue to form the neural plate, depicted by a dark streak along the dorsal axis (white arrow). However, morpholino embryos retain a large, irregular shaped yolk plug and no apparent neural plate is formed. At this stage, necrosis begins to set in (Figure 22I, arrowhead) and embryos die soon after.

To verify that the phenotype observed from morpholino injection is specific to the knock-down of Xbves protein, two control experiments were conducted. First, injection of morpholino-untargetable *Xbves* RNA was able to rescue the morpholino induced gastrulation phenotype, which is considered the gold standard for showing morpholino specificity. Second, immunohistological analysis of morpholino-injected embryos was conducted to ensure that Xbves protein was indeed knocked down. Co-injection of *Xbves* RNA lacking the 5'UTR morpholino target sequence with *Xbves* MO#1 resulted in developmentally normal embryos that are able to proceed through gastrulation (Figure 23A-D), and into tailbud and tadpole stages with minor tail malformations (Figure 23E-L, black arrows). Using our antisera against Xbves, animal caps from morpholino-injected embryos were analyzed for depletion of Xbves protein compared to uninjected embryos. The animal cap of morpholino-injected embryos were isolated at stage 9 and cultured until equivalent stage 10.5. We chose to analyze tissue sections from animal caps to reduce the excessive amount of yolk that causes autoflourescence. Caps were

fixed, cryosectioned and processed as described in Material and Methods. Figure 24 illustrates that the immunofluorescent signal from morpholino embryos is significantly reduced from that seen in sections from uninjected embryos. This finding supports the idea that morpholino injection did knock down the expression and/or accumulation of Xbves protein, as predicted. In addition, these experiments demonstrate the specificity of anti-Xbves antiserum for this gene product.

These results support our expression data that show *Xbves* mRNA and protein expression

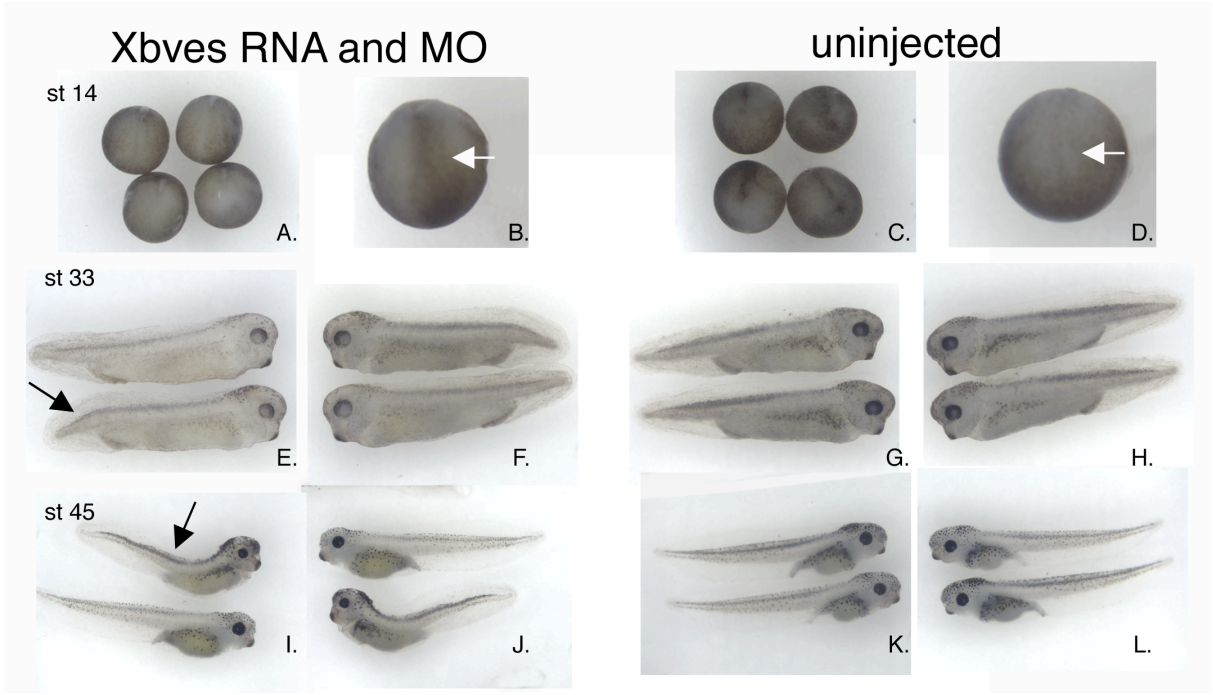

Figure 23. Co-injection of *Xbves* RNA and morpholino rescues the inhibited gastrulation phenotype. (A-D) Embryos co-injected with *Xbves* RNA lacking MO target sequence and morpholino (A-B) are able to complete gastrulation and initiate neurulation, as indicated by neural plate (white arrow), similar to uninjected embryos (C-D). Co-injected (E-F, I-J) embryos proceed to tailbud (E-F) and tadpole (I-J) stage, similar to respective uninjected embryos (G-H, K-L). White arrow points to neural plate. Note minor tail malformation in rescued embryos (black arrows).

in surface and involuting ectoderm during gastrulation. The knock down of Xbves protein in the embryo results in impaired epiboly movements during gastrulation and inhibition of continued embryonic development. Xbves role in these gastrulation movements is supported by the rescue of this phenotype with *Xbves* RNA and by a decreased signal in immunofluorescence analysis with anti-Xbves. Collectively, these data support our hypothesis that Xbves is important in epithelial migration during early embryogenesis.

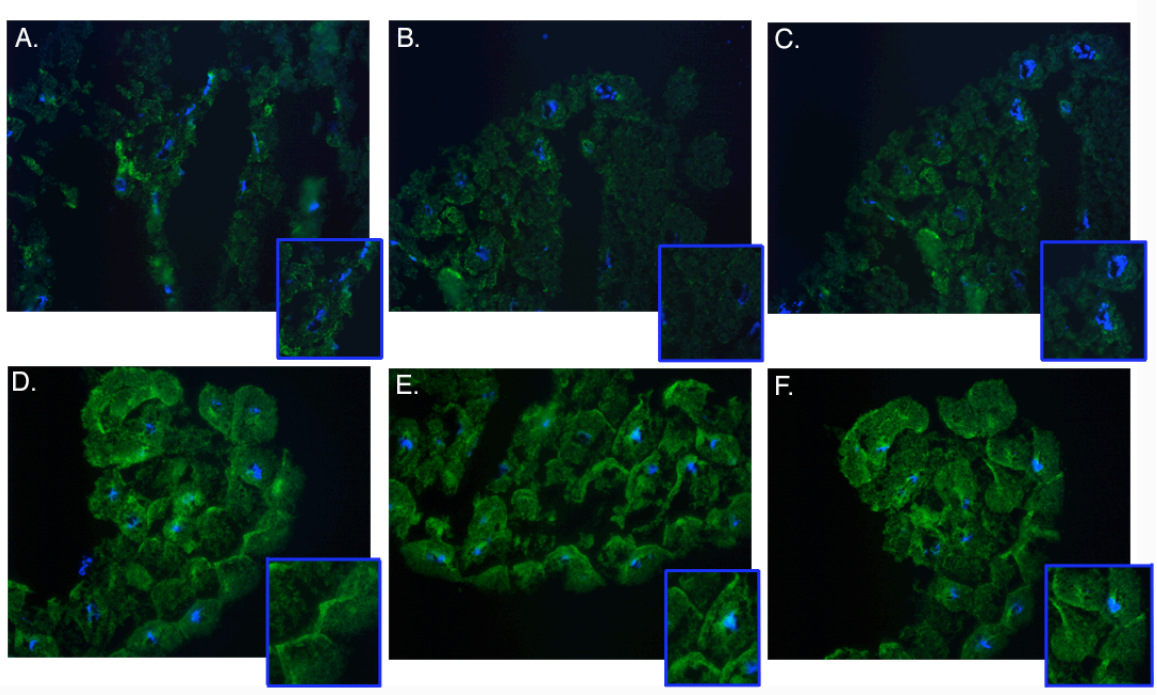

Figure 24. Immunohistochemical analysis of *Xbves* morpholino-injected and uninjected *X. laevis* embryos. (A-C) Tissue sections of animal caps extracted from morpholino-injected embryos. (D-F) Tissue sections of animal caps extracted from uninjected embryos. Insets are a 600x magnification of the respective 200x figure. These results represent n=4.

Xbves is involved in involution and epiboly but not mesoderm induction

To determine which events in gastrulation are affected as a result of decreased Xbves protein in the embryo, we examined the expression of tissue specific markers and transcripts

associated with specific developmental processes in *Xbves* morpholino-injected embryos. Migration movements of various cell populations in *X. laevis* are well documented (Hardin and Keller, 1988; Keller, 1991; Keller and Danilchik, 1988; Keller, 1980; Wilson and Keller, 1991; Winklbauer and Nagel, 1991). By tracking gene induction and progression of specific groups of cells in morpholino embryos, we can deduce the role *Xbves* fulfills in the developing embryo.

In order to examine whether organizer formation or generation of mesoderm was observed in morpholino-injected embryos, expression of the organizer specific gene, *goosecoid* (Cho et al., 1991), and an early mesoderm specific gene, *Xbra* (Smith et al., 1991), was analyzed in *Xbves* morpholino-injected embryos throughout gastrulation. During the onset of gastrulation and dorsal lip formation, no apparent differences in *goosecoid* expression exist between morpholino-injected and uninjected embryos (Figure 25A-D). At stage 10.5, *goosecoid* expressing cells involute into the deep layers of the embryo and start traveling along the dorsal axis where *goosecoid* is seen in the most anterior portions (Figure 25E-F) (Niehrs et al., 1993; Vodicka and Gerhart, 1995). A closer look at *goosecoid* expression at stage 10.5 shows an accumulation of the transcript located a distance from the dorsal lip in morpholino embryos that is half the length compared to a less intense band in the uninjected embryos (Figure 26). Bisection of these embryos reveals that what appears to be less intense band in the noninjected embryos is expression of *goosecoid* by deeper cells than the more superficial expression in morpholino embryos (Figure 29A-B). The blue streak seen in this bisected embryo represents the normal migration of *goosecoid* expressing cells from the dorsal blastopore lip anteriorly. This migration is not seen in morpholino embryos, thus resulting in an accumulation of *goosecoid* expressing cells at the blastopore lip (Figure 29A-B arrows).

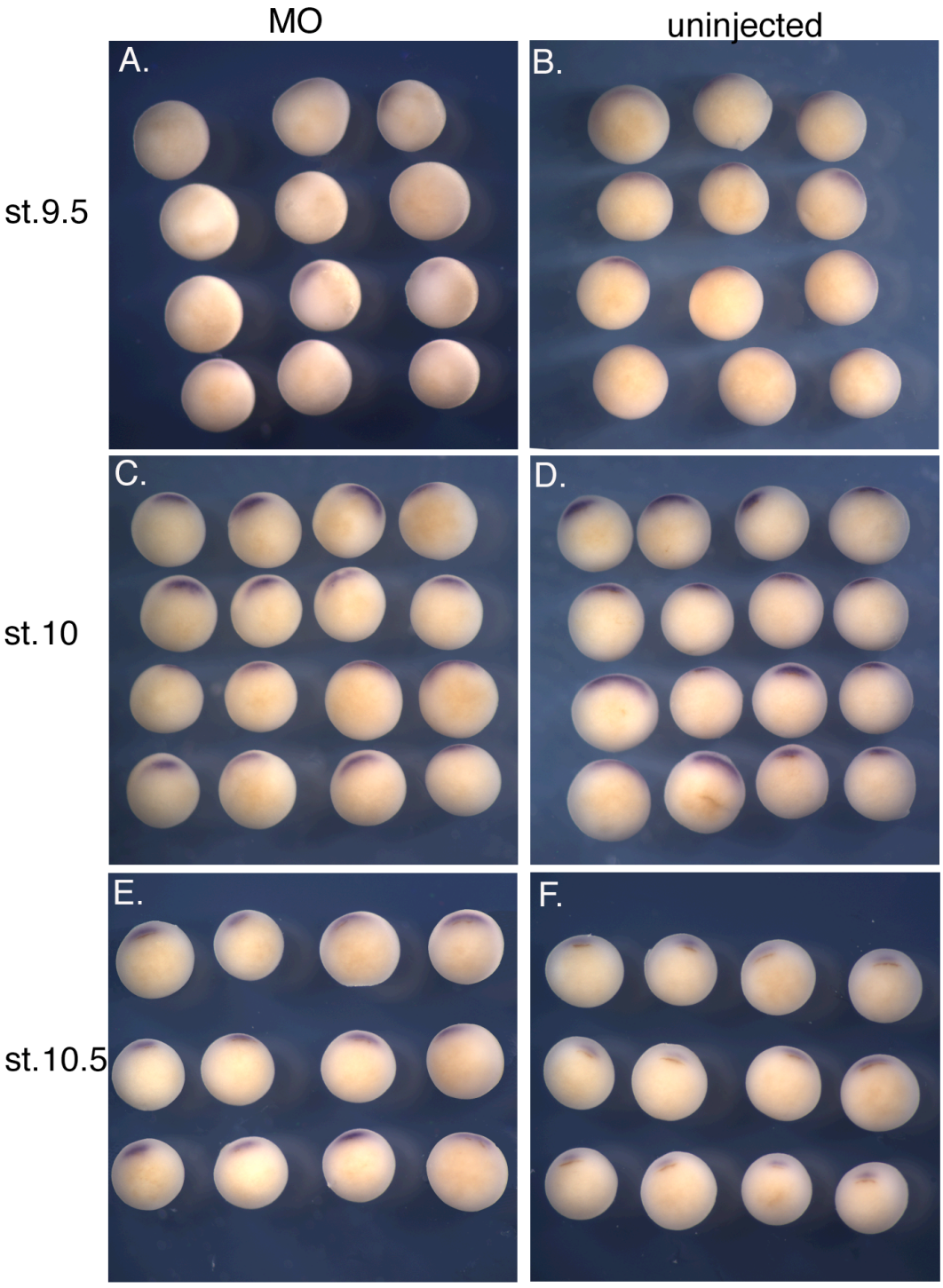

Figure 25. Detection of *goosecoid* message in *Xbves* morpholino-injected and uninjected *X. laevis* embryos. Whole mount *in situ* hybridization of *Xbves* morpholino-injected embryos (A,C,E) and uninjected embryos (B,D,F) with a probe for *goosecoid*. Embryos were injected at 2-cell stage and were fixed at stage 9.5 (A-B), stage 10 (C-D), and stage 10.5 (E-F).

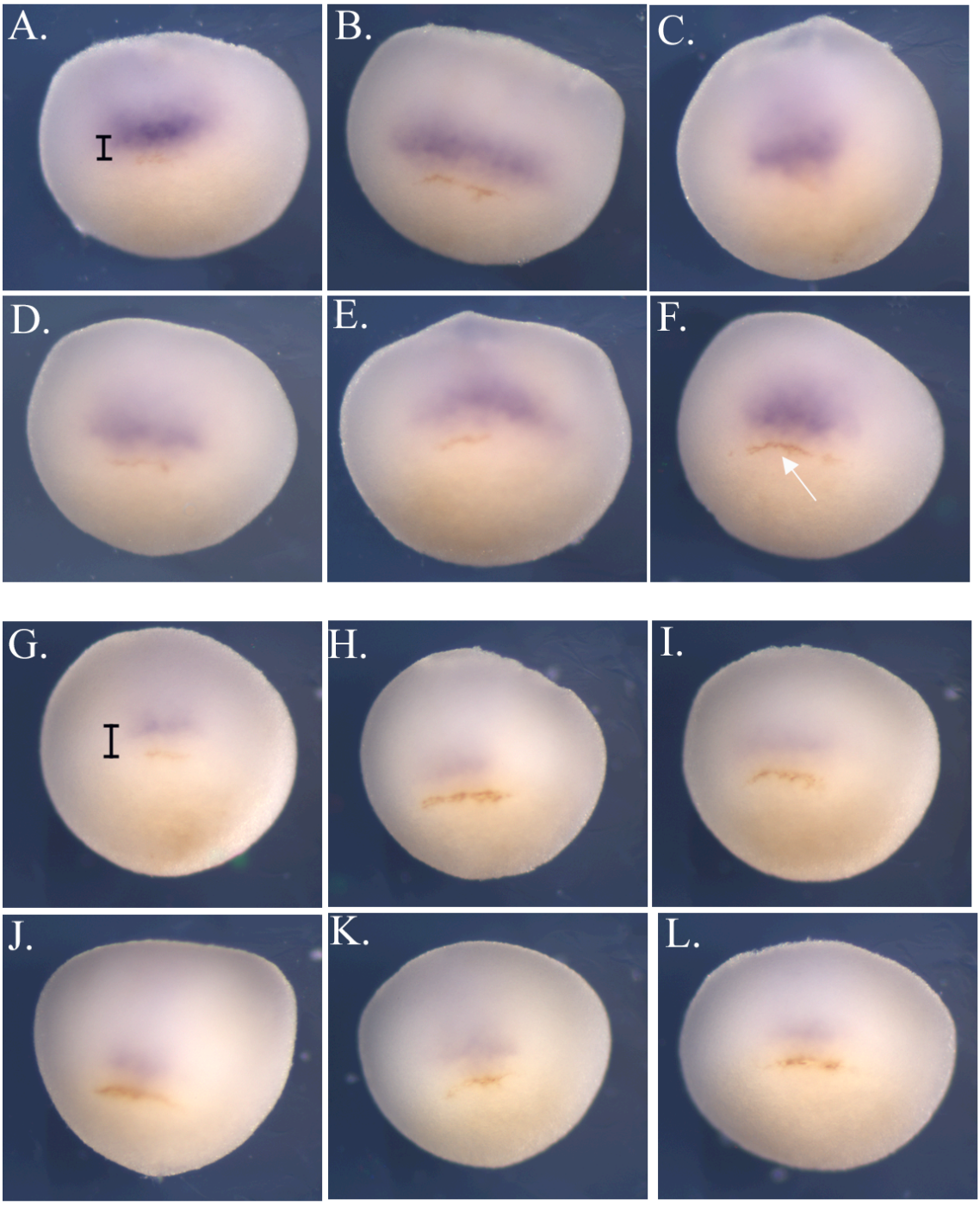

Figure 26. A closer examination of *goosecoid* expression in *Xbves* morpholino-injected and uninjected embryos at stage 10.5. (A-F) High magnification of morpholino-injected embryos shown in Figure 25E. Note the accumulation of message above the dorsal pigmented blastopore lip. (G-L) High magnification of uninjected embryos shown in Figure 25F. Note the decreased accumulation of signal above the blastopore lip. Brackets indicate distance of *goosecoid* expressing cells from the blastopore lip.

Examination of a mesoderm specific marker, *Xbra* (Smith et al., 1991), during early gastrulation in *Xbves* morpholino-injected embryos does not reveal a significant difference of expression compared to uninjected and sense control-injected embryos (Figure 27). Starting at stage 10, each set of embryos shows a concentric ring of expression at the marginal zone around the forming blastopore. However, as epiboly movements in morpholino-injected embryos are impaired and the blastopore remains large and exposed, there is an evident change in expression pattern. During mid- to late-gastrulation (stage 11-12) epiboly movements cover the blastopore and simultaneously *Xbra* expressing chordamesoderm cells involute into the embryo and travel along the dorsal axis (Figure 28B, arrow) (Cunliffe and Smith, 1992; Green et al., 1992; Kwan and Kirschner, 2003). In morpholino-injected embryos a thick, irregular ring of *Xbra* expression remains around the large blastopore but a dorsal axis pattern is not evident (Figure 28A, arrows). Bisection of these stage 12 embryos show that the noninjected embryos form an archenteron cavity (collapsed due to processing techniques), whereas morpholino-injected embryos do not (Figure 29C-D, arrowheads). It appears that the processes required for archenteron formation, involution of superficial cells resulting in a space between the yolk mass and the involuted layer and the subsequent migration into the embryo, is inhibited in morpholino-injected embryos suggesting that *Xbves* is essential for these movements.

Discussion

Bves is a member of a newly discovered gene family (Andree et al., 2000; Reese and Bader, 1999; Reese et al., 1999; Wada et al., 2001). The predicted protein products of this

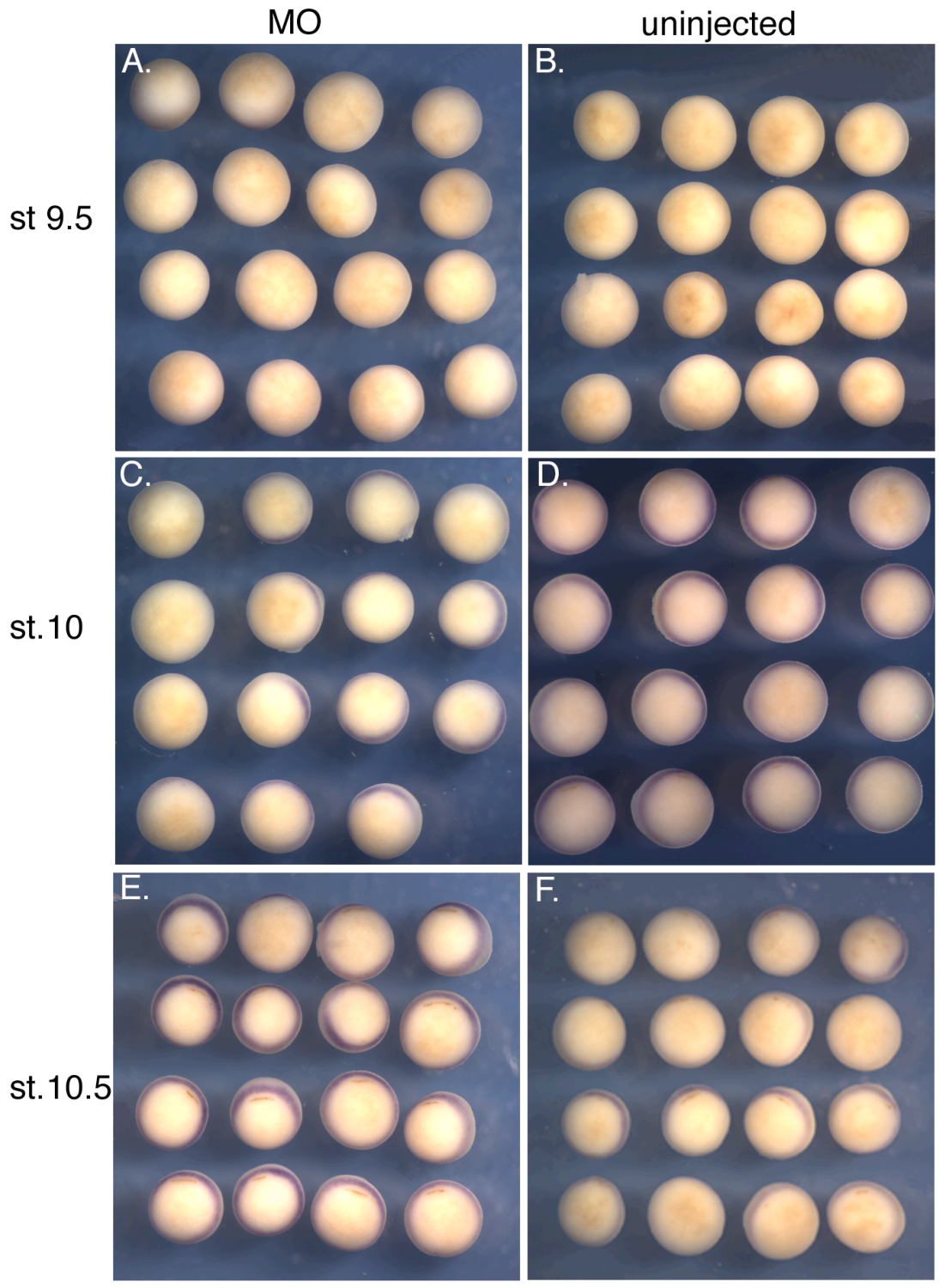

Figure 27. Detection of *Xbra* message in *Xbves* morpholino-injected and uninjected embryos. Whole mount *in situ* hybridization of *Xbves* morpholino-injected embryos (A,C,E) and uninjected embryos (B,D,F) with a probe for *Xbra*. Embryos were injected at 2-cell stage and were fixed at stage 9.5 (A-B), stage 10 (C-D), and stage 10.5 (E-F).

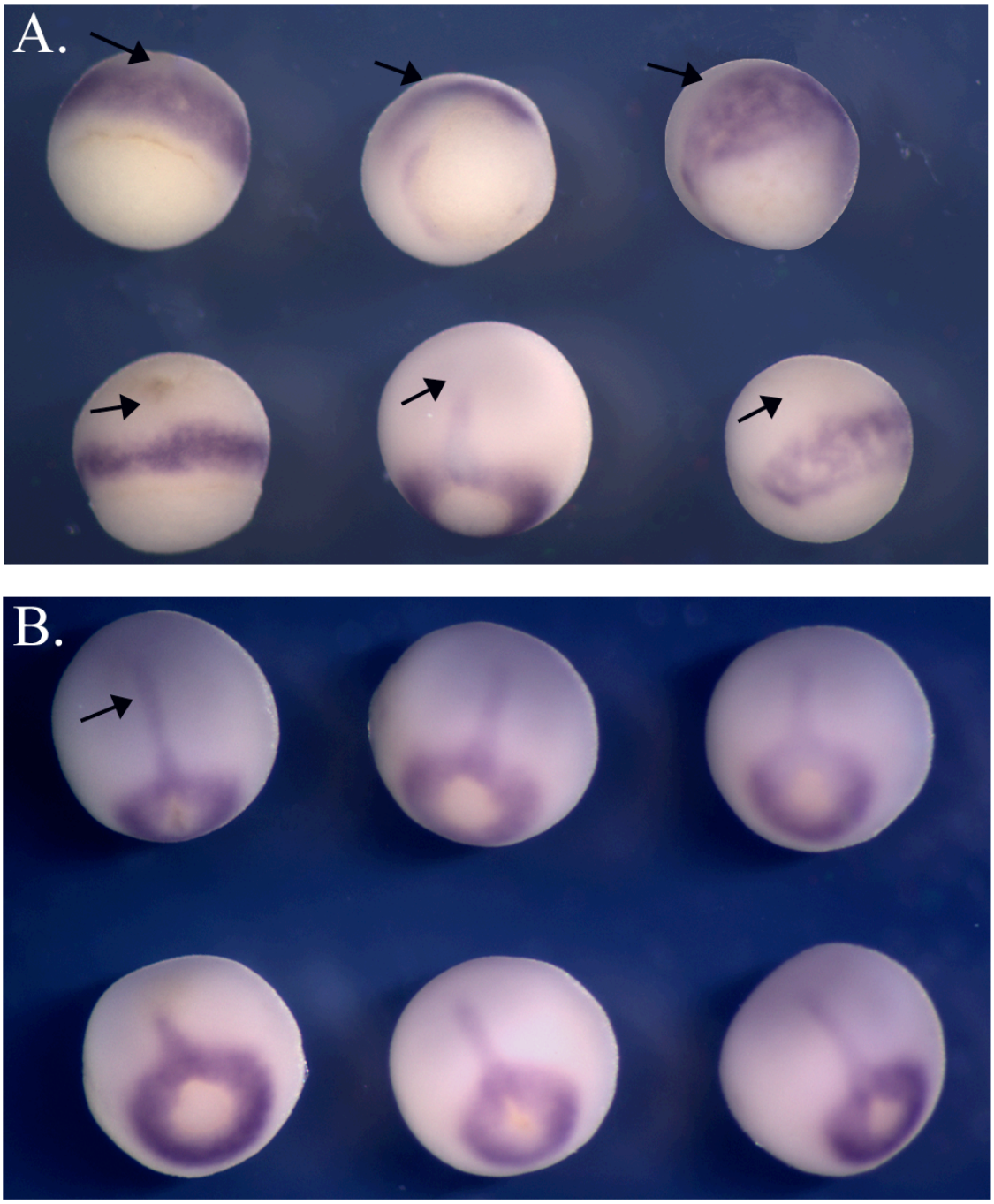

Figure 28. A closer examination of *Xbra* expression in *Xbves* morpholino-injected and uninjected embryos at stage 12. Whole mount *in situ* analysis of *Xbra* expression in morpholino-injected (A) and uninjected (B) stage 12 embryos. Black arrows point to dorsal axis of embryo. Note the large yolk plugs and lack of *Xbra* expressing cells along the dorsal axis in A.

family share no significant sequence homology with any known protein. Functional studies on these proteins are limited but suggest that Bves/Pop1a may play a role in cell-cell interaction and adhesion (Andree et al., 2002; Wada et al., 2001). Collective *in vitro* work suggests a role in epithelial adhesion and movement of epithelial sheets (Wada et al., 2001). No study in the literature describes a clear embryonic phenotype after disruption of *bves* gene product. Clearly, this is a critical element in determining the function of this molecule. I have chosen to address this issue by examining the role of *bves* in early embryogenesis using the *X. laevis* model. This allowed for examination of epithelial migration in a fundamental and manipulative system. Studies where adhesion proteins were knocked down in *X. laevis* embryos displayed a phenotype where the structural integrity of the cleaving embryo was compromised or gastrulation movements such as convergent extension or epiboly was inhibited (Heasman et al., 1994b; Kuhl et al., 1996; Lee and Gumbiner, 1995; Levine et al., 1994). According to published *bves* studies and studies performed in *X. laevis,* I deduced that I could use the *X. laevis* and morpholino technology to test my hypothesis that *Xbves* plays an essential adhesive role in the migrating epithelium. The present data are the first to demonstrate that disruption of Xbves function inhibits epithelial cell movement during early development and a failure to complete gastrulation.

***Xbves* is expressed during early development**

No one study has employed both molecular and immunochemical reagents to analyze the expression of *bves/pop* gene products in any one organism during development. In addition, previous studies have varying reports on the distribution of *bves/popeye* gene products in developing vertebrates

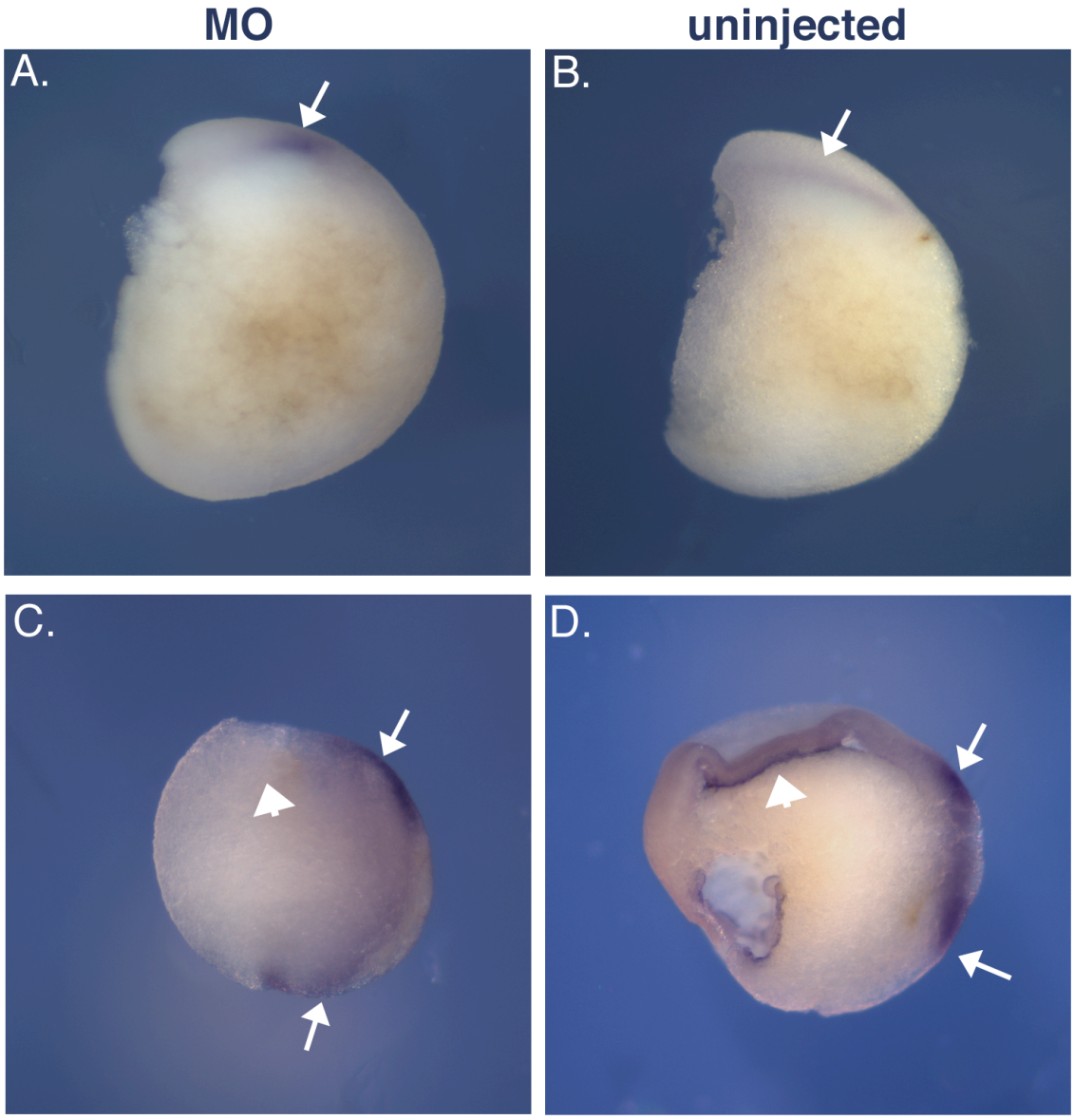

Figure 29. Bisection of *goosecoid* and *Xbra in situ* hybridized morpholino-injected and uninjected embryos. (A-B) Stage 10.5 morpholino-injected (A) and uninjected (B) embryos (from figure 14) were bisectioned along the dorsal axis. White arrow point to *goosecoid* expression. Note the uniform streak of *goosecoid* from the blastopore lip along the dorsal axis anteriorly in B compared to the large accumulation at the blastopore lip and little anterior expression in A. (C-D) Stage 12 morpholino-injected (C) and uninjected (B) embryos (from figure 16) were bisectioned along the dorsal axis. White arrows identify the edges of the yolk plug. Note the distance between the two and the uneven *Xbra* staining at these regions in C. The white arrowhead points to the archenteron in D and indicates the absence of one in C.

(Andree et al., 2002; Andree et al., 2000; DiAngelo et al., 2001; Hitz et al., 2002; Reese et al., 1999; Vasavada et al., 2004; Wada et al., 2001). Therefore, in prelude to testing *Xbves* gene function, it was necessary to determine the temporal and spatial distribution of its products over a specific period of embryonic development. In the current study, cDNA cloning, EST database searches, *in situ* hybridization, RT/PCR and immunofluorescence analyses demonstrate the presence of *Xbves* mRNA and protein in the early frog embryo. During this period of time, *Xbves* mRNA and protein are broadly expressed in the animal cells both before and during the epithelial movements leading to the formation of the blastopore and further gastrulation movements. As development proceeds, Xbves protein is observed in newly formed mesoderm. A previous *in situ* hybridization study suggested that *Xbves/pop1a* expression during early development is "uninformative" and that later expression is confined to the heart (Hitz et al., 2002). Therefore these additional and extensive analyses were necessary. It is possible that procedural variations including probe preparation and colorimetric development account for the variation in the results. Still, all the present data support the premise that *Xbves* RNA and protein are present in the early *X. laevis* embryos.

Additionally, data from our laboratory demonstrate the adhesive nature of Bves protein in the early *X. laevis* embryos and its early trafficking to points of cell-cell contact during epithelial sheet formation and repair (Ripley et al., in press). Andree et al. (2002) have suggested that *bves/pop1* plays a role in the fusion of skeletal myoblasts during muscle regeneration. From these data, we hypothesize that Bves plays a role in cell-cell interaction and adhesion. While it was not possible to determine the distribution of the protein during the earliest phases of cleavage, Xbves appears at the cell periphery of the blastula and gastrula (Figure 18). Additionally, *Xbves* transfected L-cells display adhesive behavior. These data correlate to our

previous studies in avians and mammals and are consistent with a function for this protein at the cell surface (Reese et al., 1999; Wada et al., 2001; Wada et al., 2003). Later, Xbves expression is limited to specific populations of epithelial cells and striated muscle. Thus, while initial studies of *bves* show high levels of expression in heart and skeletal muscle we show that *Xbves*, like other adhesion gene products, is more broadly expressed in early embryogenesis and may function in a more diverse set of cells.

Bves has an essential role in epithelial movement during early amphibian development.

Treatment of embryos with *Xbves* morpholino antisense oligonucleotides results in an arrest of development during gastrulation. This phenotype is typified by the lack of epithelial migration required to cover the yolk plug and a halt in the involution of superficial cells into the deeper layers. Embryonic development can be largely rescued with an *Xbves* transcript modified to escape morpholino blockage suggesting that this protocol does test Xbves function in these events.

The current study demonstrates that *Xbves* plays an important role in early *X. laevis* development. Specifically, knock-down of *Xbves* protein results in the lack of migration during epiboly and involution but not mesoderm induction. Our interpretation of these results is that disruption of Xbves function leads to improper migration of epithelial cells during this period of time, leading to a failure in yolk plug closure and defects in the formation of the archenteron and notochord. Xbves protein is observed at the cell membrane of cultured A6 cells and is seen at the periphery of embryonic cells when we can first visualize the protein during cleavage. In addition, L-cell aggregation assays with Xbves demonstrate the conserved nature of Bves adhesive properties. Thus, disruption of epithelial movement during early embryonic

development is not unexpected with alteration of proteins involved in epithelial cell adhesion. Furthermore, this series of morpholino knock-down experiments suggests that Xbves is a vital molecule involved in gastrulation movements. It is imperative that these cells maintain and migrate as an epithelium for proper cell-cell communication and migration during gastrulation.

Before gastrulation begins, a subset of cells must be properly arranged in the embryo by a group of pregastrula movements. Animal cells constituting the blastocoel roof need to partially cover the vegetal hemisphere in a movement called pregastrula epiboly. During this process it is necessary that epithelial junctions between these animal cells be preserved to prevent the inner cells from intermixing with the animal cells. In order for these cells to increase the surface area needed to cover the vegetal hemisphere the animal cells must "interdigitate by radial intercalation", which allows the multi-cell layer to form a single-cell inner layer of the blastocoel roof. This process also allows for some of the cells from the blastocoel roof to be pushed into the subequatorial region and form a multilayered ring.

Gastrulation movements begin with the continuation of epiboly that started during late blastula stage. Additionally, as these cells extend vegetally, they interdigitate circumferentially in a process called convergence. Concurrently, the noninvoluting marginal zone is stretched in an animal-vegetal direction, called extension. At the future dorsal side of the embryo, a small group of prospective local endodermal cells, called bottle cells, elongate and constrict their apices to invaginate into the embryo at the marginal zone to form a blastopore. Next, cells from the marginal zone travel over the blastopore lip, involute inward into the embryo and travel along the blastocoel roof. The bottle cells that are the first cells to pass into the embryo line the archenteron and will become the pharyngeal cells of the foregut. The next group of involuting cells is the chordamesoderm cells that will form the notochord. This stream of cells into the

embryo eliminates the blastocoel and forms a new cavity called the archenterons, resulting in a third germ layer, mesoderm, situated between prospective endoderm and ectoderm. The movements of epiboly, convergent/extension and involution together allow the formation of the mesoderm as well as the animal cells and noninvoluting marginal zone to cover the entire surface of the embryo.

Our studies clearly show that *Xbves* is expressed both during blastula and gastrula stages, thus suggesting a functional significance of this gene product during these times. Morpholino knock-down studies show a halt in the progression of gastrulation, leaving a large, irregular shaped exposed yolk plug. From our knowledge of gastrulation movements described above, the resulting *Xbves* morpholino phenotype correlates with the inhibition of gastrulation movements, specifically epiboly, or the inability of animal cap cells to cover the vegetal pole. The detection of an organizer specific marker, *goosecoid* and a mesodermal specific marker, *Xbra,* in these morpholino-injected embryos suggests that inhibition of gastrulation is not due to lack of organizer formation or a disruption in mesoderm induction. Instead, our hypothesis is confirmed that the knock-down of *Xbves* in *X. laevis* embryos results in impaired cell migration leading to the arrest of development. This is illustrated by monitoring the expression of *goosecoid* and *Xbra* during gastrulation in both *Xbves* morpholino-injected and uninjected embryos.

The organizer specific *goosecoid* transcript accumulates in the dorsal mesodermal precursor cells located in the deep layers directly above the dorsal blastopore lip. As these cells involute *goosecoid* is seen at the leading edge of the migrating mesoderm and is localized in the most anterior portions (Niehrs et al., 1993).

During early gastrulation *Xbra* is expressed in presumptive mesodermal cells located at the marginal zone. This expression pattern appears normal in both uninjected and morpholino-

injected embryos. However, upon dorsal blastopore lip formation when *Xbra* expressing chordamesoderm cells involute into the embryo and travel along the dorsal axis anteriorly forming the notochord, this process is disrupted in morpholino-injected embryos (Figure 28). Late gastrula Xbves depleted embryos show an unusually wide band of mesodermal cells around the blastopore, but migration of chordamesoderm along the dorsal axis is not evident. These morpholino-injected embryos remain at this state until they necrose.

Therefore, based on the phenotype of *Xbves* morpholino-injected embryos and the distinctive *Xbra* and *goosecoid* expression patterns described, I conclude that Xbves is required for epithelial cell-cell adhesion required for proper cell migration during gastrulation. Currently, it can be deduced that epithelial movement is inhibited, but the exact mechanism is unknown. It's possible that the balance of cell adhesion and cell malleability is disrupted. This may cause increased adhesion and lack of movement or inhibition of coordinated sheet expansion. Future studies focusing on expression of the various junctional proteins and cell junction complex formation in Xbves knock down embryos will clarify the role of Xbves in epithelial cell-cell junctions during gastrulation movements.

CHAPTER IV

BVES IS EXPRESSED IN THE EPITHELIAL COMPONENTS OF THE EYE AND REGULATES CORNEAL REGENERATION

Introduction

The dynamic subcellular expression pattern and epithelial function of *bves* is not restricted to gastrulation movements. Previous data has shown *bves* expression in a number of developing organ tissues (Andree et al., 2000; Reese et al., 1999; Wada et al., 2001), suggesting a function in these developmental processes as well. Although *bves* expression in the eye has not been reported, it is not surprising that *bves* plays a role in a developmental process that involves dynamic morphogenetic movement and reshaping of epithelia. The first evidence of *bves* expression in the eye was from an immunofluorescence analysis I performed in *X. laevis* tadpoles to characterize the Xbves antiserum and verify reported expression patterns in this species. Results from this initial immunofluorescence study show Bves expression in the *X. laevis* lens and outer layer of the retina; however, the cornea was not included in this tissue section (figure 20F). Furthermore, in an attempt to titrate *Xbves* morpholino concentrations, injection of lower concentrations (compared to amount injected to generate gastrulation phenotype) of morpholino antisense oligomer generated embryos that proceeded through gastrulation, but displayed developmental abnormalities. The most notable abnormality was an absence of or underdeveloped eye (discussed in detail in dissertation discussion). Therefore, the combined *Xbves* expression pattern and morpholino data suggested a vital function in eye development and warranted further studies of *bves* in this process.

This chapter will first outline the general morphogenetic movements that occur during retina, lens, and cornea formation. I will then show *bves* expression in the formation of each of these structures. Lastly, I will describe experiments that take advantage of the propensity of human corneal epithelial cells to grow and wound heal in culture. *Bves* morpholino treatment of these cells will be examined. Results will show that *bves* is expressed in specific epithelia that will differentiate into the major structures of the eye, and that Bves protein is necessary for the proper migration and cell-cell adhesion of corneal epithelia. These studies further support our initial hypothesis that Bves plays a role in cell migration and morphogenesis during embryogenesis.

Development of the eye requires a complex series of differentiative events. Establishment of the three main eye primordia, the retina, lens and cornea, involves movement and reshaping of embryonic epithelia (Pichaud and Desplan, 2002; Tripathi et al., 1991). Additional contributions of mesenchymal cells derived from head mesoderm and neural crest are also essential for proper eye development (Beebe and Coats, 2000; Hsieh et al., 2002). The formation of this complex organ begins with the lateral evagination of the neuroectodermally-derived diencephalon of the brain, forming the optic vesicle. The epithelial optic vesicle then invaginates forming a bilayer optic cup, bringing inner and outer retinal layers to face each other (Figure 30). The inner layer of the cup will differentiate into the neural retina, while the outer layer will form the retinal-pigmented epithelial layer (RPE) (Cepko et al., 1993; Livesey and Cepko, 2001). Together these two layers will fuse and form the mature ten-layered retina.

The formation of the lens begins with a signaling event from the optic vesicle to the head ectoderm (Henry et al., 2002; Jean et al., 1998). A population of surface epithelial cells divides and elongates, forming a local thickening of epithelium called the lens placode (Figure 30). This

placode starts to lose contact with surrounding epithelium and begins to drop into the optic cup, forming the lens pit, and subsequently pinching off the surface to form the rounded lens vesicle. The lens vesicle consists of a ring of epithelial cells that is divided into an anterior portion that

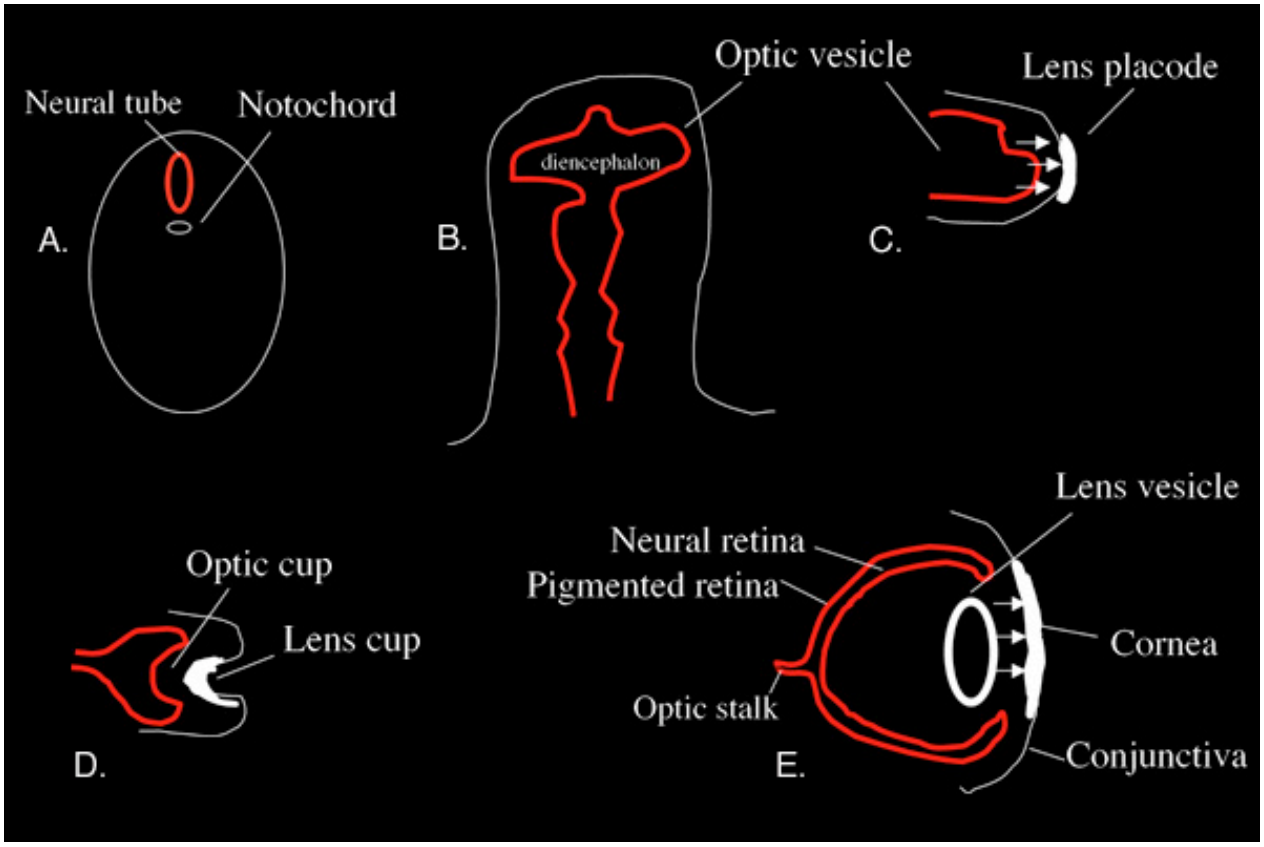

Figure 30. Illustration of the major morphological events during retina, lens and cornea development and the epithelial movements required for this process. (A) A cross-section through the developing neural tube shows the position of the surface ectoderm, neural tube and notochord. (B) A longitudinal diagram shows the diencephalon bulging toward the surface ectoderm forming the optic vesicle. (C) This diagram illustrates signaling (arrows) from the optic vesicle and the response of the surface ectoderm to form the lens placode. (D) The invagination of the optic vesicle leads to the formation of the optic cup with inner, neural and outer, pigmented layers. The lens cup is also formed by invagination of the placode. (E) The lens vesicle is surrounded by the developing retina after the lens vesicle loses contact with surface ectoderm. Finally, additional signals from the lens (arrows) induce formation of the cornea from surface ectoderm.

will remain undifferentiated, and a posterior half that will differentiate into primary fiber cells (Reed et al., 2003). As development continues, the anterior epithelium remains proliferative and provides cells that migrate towards the equator, called the bow region or the transition zone, of the lens and exit the cell cycle to begin differentiation into secondary fiber cells (Dahm et al., 2003; de Iongh et al., 2001). These fiber cells elongate and form multiple, concentric layers of the primary fiber cell center. As these fibers grow they produce large amounts of crystalline and their cell nuclei are expelled (Bower et al., 1983; Brady et al., 2001). This dynamic process of epithelial migration and differentiation continues throughout adulthood.

The development of the cornea shares some similarity with lens formation. A population of cells within the surface epithelium responds to a signal that remains unresolved to form a cornea placode (Beebe and Coats, 2000). Corneal epithelium first produces connective tissue composed of collagen I and II called the primary stroma in chick embryos (Meier, 1977). Cells of the neural crest subsequently migrate into the space beneath the corneal epithelium, take on mesenchymal characteristics, and produce the secondary corneal stroma and endothelium (Hsieh et al., 2002; Reneker et al., 2000). In mammals, production of primary stroma may not be a distinct event (Chiambaretta et al., 2002). As development proceeds, the corneal epithelium expands from a single cell layer into a stratified epithelium. The developmental stage at which stratification takes place varies in a species-specific manner. In addition, diversification of surface epithelium into cornea, limbus, and conjunctiva is accompanied by differential gene expression (Wang et al., 2002; Xu et al., 2002). The mature cornea consists of a multilayered epithelium, a thick collagen filled stroma, and a single cell layer of endothelium.

A shared property in the development of the retina, lens and cornea is that each structure originates in part from an epithelium. In all three cases, the original epithelium undergoes

dramatic morphogenetic changes that depend on proper reshaping of the original cell layer while maintaining epithelial polarity and integrity. The formation and reshaping of epithelia is dependent on cell-cell interaction via a complex set of adhesion molecules (Leong et al., 2000; Liu et al., 2002; Sugrue and Zieske, 1997; Wedlich, 2002). In large part, tight, adherens, and desmosomal junctions are responsible for maintaining cell adhesion and polarity in mature epithelia (D'Atri and Citi, 2002; Kojima et al., 2001), but components of these structures often intermix during epithelial morphogenesis (Leong et al., 2000; Sugrue and Zieske, 1997). Resolution of the distribution of adherent proteins during eye development is essential for an understanding of their function in this process. While it is clear that epithelial adhesion and movement are critical for eye development, little is known about the role of specific cell adhesion molecules in eye morphogenesis.

The present study explores the role of a novel cell adhesion molecule, Bves/Pop1a, in the formation of the retina, lens and cornea. We originally isolated *bves* (blood vessel/epicardial substance) from a heart specific subtraction screen and showed expression in the epicardium and coronary smooth muscle using our first generation of antisera (Reese et al., 1999). Subsequently, Andree et al. (2000) identified two or three genes they termed *popeye* in chickens, mice and humans. The *bves* transcript and gene are identical to *pop1a*. In that study, analysis of RNA expression showed that the *bves/pop1a* transcript is expressed at high levels in cardiac and skeletal muscle by *in situ* hybridization and RNA blot analyses. DiAngelo et al. (2001) demonstrated protein expression in cardiac muscle of the developing chicken using a monoclonal antibody. The Human Gene Nomenclature Committee, NCBI and Mouse Genome Informatics have designated this gene product as “Bves” and we use this term henceforth in this report.

Our previous data suggest that Bves regulates cell-cell interaction in a calcium-independent, homophilic manner when transfected into non-adherent cells (Wada et al., 2001; Wada et al., 2003). The molecule has three conserved transmembrane domains that are essential for insertion and/or retention in the membrane. While Bves proteins share no homology to any other known protein family, the members within the family and across species are highly conserved in amino acid sequence (Andree et al., 2000; Reese and Bader, 1999; Reese et al., 1999). A recent study by Andree et al. (2000) observed no developmental abnormalities or phenotypes after ablation of the *pop1* gene. However, they did note a delay in skeletal muscle regeneration in these mice and suggested that this may be due to a problem in cell-cell interaction. Thus, while *in vitro* analysis of cell behavior suggests a role in cell-cell adhesion or interaction, the role of this gene family in development and repair is only now being investigated.

There are several lines of evidence to suggest that *bves* expression extends beyond heart and skeletal muscle. First, RT/PCR analysis in Andree et al. (2000) shows a broad distribution of expression in the developing heart, skeletal muscle, lung, kidney, brain, and spleen of the mouse embryo but not to the levels detectable by *in situ* or RNA blot analysis. Additionally, although not noted in the text, mRNA expression is clearly seen in the endoderm of the developing gut by *in situ* hybridization (figure 4 of Andree et al., 2000). In addition to these studies, numerous ESTs have been reported for non-striated cell types in many organisms (NCBI). Using a second set of monoclonal, polyclonal and single chain antibodies, our group has reported Bves expression in other epithelial structures as well as skeletal muscle and cardiac muscle (Wada et al., 2001; Wada et al., 2003) and in the three embryonic germ layers of the developing chicken embryo (Osler and Bader, 2004).

These previous data led us to examine the expression pattern of Bves in developing embryos, with special reference to epithelia that contribute to organs or organ systems. The eye provides a unique developmental system where its three major and divergent components, the retina, lens and cornea, are derived from epithelial sources. These epithelia display complex morphogenetic movements that are essential for generating the adult structure. In addition, in the case of the cornea, regeneration of the epithelium entails the migration of adjacent surviving cells over the wound to replace lost cells and serves as an example of epithelial morphogenesis in the adult organism. In the present study, we show that Bves is expressed in all three epithelial progenitor populations of the eye but in unique subcellular locations. In addition, using an *in vitro* model of corneal wound healing, we observed that Bves staining is lost at the surface of cells advancing from the wound edge. Later, as epithelial continuity is established, Bves is again seen at the cell surface. In an initial effort to elucidate Bves function in the eye, we conducted an anti-sense morpholino study to "knock down" Bves protein expression in cultured corneal epithelium. This methodology has proven to be an effective method for disruption of protein function (Heasman et al., 2000; Heasman et al., 2001). We observed that morpholino treatment of uninjured corneal epithelium led to irregularities in cellular sheet formation. Upon injury, morpholino-treated corneal cells move more rapidly into the wound area as compared to non-treated cells. Still, these cultures did not produce an intact monolayer of epithelial cells in the wound area as compared to control cultures. We discuss the implications of these experiments in reference to the possible role of Bves in cell-cell interaction and epithelial integrity.

Materials and Methods

Embryo/Tissue Collection and Cell Culture

White Leghorn fertilized embryos were obtained from Truslow Farms (Maryland) and incubated in a high humidity 37˚C chamber. Embryos were collected and staged according to Hamburger and Hamilton (Hamburger and Hamilton, 1992). Staged Black Swiss mice were sacrificed and the eyes removed for tissue sectioning as described below. A SV40-immortalized human corneal epithelial cell line was obtained from the laboratory of Dr. Karou Araki-Sasaki (Araki-Sasaki et al., 1995) and cultured at 37 ˚C in a defined serum-free keratinocyte medium (Gibco).

Antibodies

The B846 polyclonal antiserum was developed in rabbits (Biosynthesis) against the C-terminal tail of Bves1 (DPTLNDKKVKKLEPQMS; amino acids 266-283 of mouse Bves) followed by affinity purification with a peptide-conjugated column (Reese et al., 1999). This serum has been shown to be reactive with the Bves protein produced from the cloned mRNA and cross-reacts with several avian and mammalian species (Reese and Bader, 1999; Wada et al., 2001). In addition, the antiserum has been shown to be specific for Bves protein using immunopeptide competition (see below) and transfection analysis (Osler and Bader, 2004). Monoclonal antibodies against various junctional complex proteins were purchased as follows: β-catenin (Sigma, C-7207), E-cadherin (Transduction Laboratories, 877-232-8995), ZO-1 (Zymed, 33-9100), and 3F11, anti-Pop1/Bves (NIH Hybriboma Bank).

Immunohistochemistry

Embryos and tissue were collected in PBS and incubated in 30% sucrose for two hours. Samples were embedded in OCT, frozen in dry ice/ethanol bath, and 5 μm sections were cut on a cryostat. Sections were fixed in 70% methanol for 5 minutes, rinsed with PBS, permeablized with 0.25% Triton X-100 and blocked in 2% bovine serum albumin/PBS for 1 hour at room temperature. Sections were co-incubated with the B846 Bves antibody and antibodies directed against other junctional proteins overnight at 4˚C. The sections were washed 3 times with PBS and incubated with appropriate secondary antibodies (Jackson Laboratories) and DAPI for at least 4 hours at room temperature in the dark. Images were captured on an Olympus fluorescent microscope and digital camera using Magnafire Optronics. Negative controls included incubation with no primary antibody, non-reactive primary antibody and peptide competition. For peptide competition, the 3' DNA sequence coding for the C-terminal 289 amino acids were cloned in-frame into pGEX and used to produce recombinant protein using published techniques (DiAngelo et al., 2001). Purified protein was reacted with affinity-purified antiserum in PBS at 100, 50, and 10 fold molar excess along with no added peptide for 4 hours at 4˚C. Following this reaction, the solution was transferred to sections of day 7 chick eyes and incubated overnight at 4˚C. Sections were then processed for indirect immunofluorescence using standard techniques detailed above. Images are captured and processed identically for comparison between control and experimental groups. Corneal epithelial cells were grown on glass chamber slides, rinsed with PBS, fixed in 70% MeOH and permeablized with 0.1% Triton. Similar peptide competition experiments as described above were conducted on cultured corneal epithelial cells to determine the level of background staining in this particular experimental method. Immunofluorescence analysis of these cells was completed as described for tissue sections.

RT/PCR Analysis

RNA was isolated using Trizol reagent from whole eyes and hearts at selected stages and subjected to RT/PCR analysis. The entire eye was dissected and thus the values presented can only be ascribed to expression in the entire eye and not to any specific cell type within the structure. Tissues were isolated under sterile conditions and extracted using Trizol reagent according manufacturers directions. RNA concentrations were quantified and reacted with primers for *GAPDH* and *bves*. Sequences for these primers and PCR conditions are given in Osler and Bader (2004). Controls with no reverse transcriptase (RT) were conducted to ensure the RNA-dependence of the reaction. Products were analyzed on 1% agarose gels.

Morpholino "Knockdown" of Bves Expression and Wound Healing

SV40-immortalized human corneal epithelial cells were plated at a seeding density of 20,000/cm^2. Typically, the cells reached full confluence by day 6. Injury was induced by a scratch injury or by application of modified drill press under sterile conditions (Lambiase et al., 2000; Pancholi et al., 1998). Cultures were returned to the incubator and grown for selected time periods. Cultures were fixed and processed for immunofluorescence as described above. Two morpholino anti-sense oligonucleotides for human *bves1* were synthesized and applied to cultures using the manufacturer's methods (Gene Tools). The sequence of the morpholino that gave the strongest phenotype was 5' ATCTTTCTTATACCTGGATGTGCAG 3'. Control morpholinos recommended by the manufacturer were used to test the possible non-specific effects of morpholino delivery on Bves expression. In addition, fluorescenated control morpholinos for mouse LEK1 (Ashe et al., 2004) were applied to cultures to determine the efficiency of morpholino uptake. The percentage of cells taking up this morpholino was

approximately 20-30 % using these cells. In one series of experiments, the possible effects of Bves morpholino knockdown on epithelial integrity were tested. In these experiments, morpholinos were applied to cells at day 3, (40-60% confluence) and at day 5 (80-90% confluence). Cultures were maintained after application and monitored daily for possible changes in epithelial morphology. In these studies, control and experimental morpholino-treated cultures were processed for immunochemical analysis with B846 and control antibodies to detect changes in Bves expression and in the structure of the intact epithelium. In a second set of experiments, control and morpholino-treated cultures were wounded using a modified drill press as described above and the rate of cell movement into the wound space was monitored by phase microscopy. Again control and Bves anti-sense morpholino was applied twice, at day 4 (50-70% confluence) and immediately after "injury" to the fully confluent culture (day 6). The defect area was monitored daily by using light phase microscopy. A digital image of the defect area was record at 10x magnification. The original wound area was obtained by using Image J software (NIH). The amount "healing" or formation of new epithelium in each wound was determined by the following formula: (1 – surface area at day X /surface area day 0) and reported as percentage growth. Single tail Student's T-test was applied to determine the possible significance of values in these three groups (n=7).

Results

Bves expression in the eye

In an initial survey of Bves expression during embryogenesis, we determined that Bves staining was observed in elements of the developing eye, most prominently in its epithelial precursors of the cornea, lens and retina (Figure 31). These data led us to conduct an analysis of

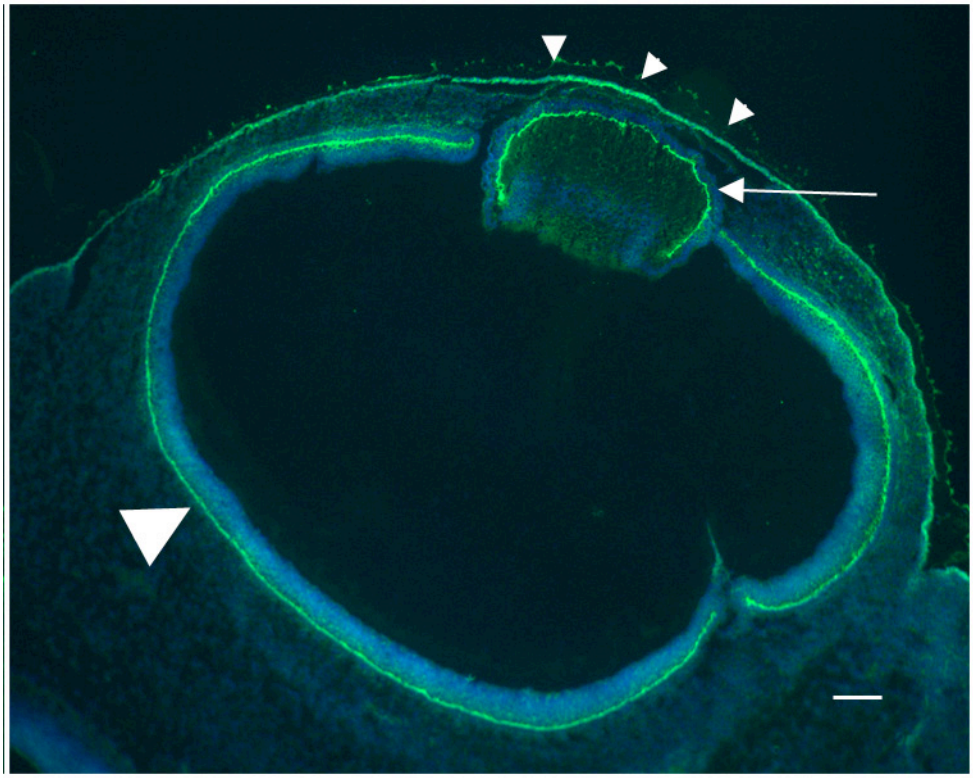

Figure 31. Identification of Bves protein in the developing eye. Bves expression in the developing chick cornea (small arrowheads), lens (arrow), and retina (large arrowhead) at day 4 was detected with B846 antiserum (green). DAPI (blue) was used to stain nuclei. Scale bar = 100 um.

Bves expression in the eye at selected stages of development. In the following studies, we have primarily used the chick as a developmental model for eye formation due to the ease in obtaining embryos, but we also conducted similar analyses on mice and frogs. Experiments with frogs were conducted with antisera specific to the frog protein and will be reported elsewhere (Ripley,

Wright and Bader, unpublished data). The same general pattern of Bves expression presented below was observed in these three classes of vertebrates indicating conservation of Bves expression in avian, mammalian and amphibian eye development.

To demonstrate that *bves* mRNA was present in the developing eye, RT/PCR analysis was conducted on selected stages of eye development in the chick. Heart tissue was also analyzed as a positive control for expression. RT/PCR analysis was chosen because previous studies indicated that RNA transcripts may not be expressed at levels detectable by standard *in situ* hybridization or northern blot analysis (Andree et al., 2000). In these studies, the entire eye was dissected, and thus the resultant reaction products reflect expression throughout the eye at the indicated stage. As seen in figure 32A, a discrete reaction product of the predicted size was obtained with RNA isolated from day 2 head region and day 6, day 18 and day 21 embryonic chicken eyes. A product at the same mobility was observed using RNA isolated from hearts at selected stages of development but was not observed in controls without reverse transcriptase (RT) (data not shown). The GAPDH reaction serves as a positive control for RNA input (Figure 32A). It should be noted that abundance of message from the eye is similar to that observed from the heart in this assay system. Andree et al. (2000) also demonstrated relatively high levels of RT/PCR product in tissues other than heart and striated muscle.

A series of peptide competition experiments were conducted to test specificity of B846 for Bves. As seen in figure 32B.a, antiserum B846 reacts with cells of the developing retina at day 7 of embryonic development (to be discussed in more detail below). Peptide competition at 100 molar excess completely eliminated B846 antibody reactivity in sections of the day 7 retina (figure 32B.b). Lesser concentrations of competing peptides also blocked anti-serum reactivity. No primary antibody controls also showed no staining for these sections (figure 32B.c). These